Optics & Laser Technology 44 (2012) 1551–1555

Contents lists available at SciVerse ScienceDirect

Optics & Laser Technology

journal homepage: www.elsevier.com/locate/optlastec

Heating process and damage threshold analysis of Au film coated on Cu substrate for femtosecond laser

Tingfeng Wang [a], Jin Guo [a], Junfeng Shao [a], Tao Sun [a], Anmin Chen [a,b,*], Hang Liu [b,*], Dajun Ding [b]

[a] State Key Laboratory of Laser Interaction with Matter, Changchun Institute of Optics, Fine Mechanics and Physics, Chinese Academy of Sciences, Changchun 130033, People's Republic of China

[b] Institute of Atomic and Molecular Physics, Jilin University, Changchun 130012, People's Republic of China

ARTICLE INFO

Article history:
Received 31 August 2011
Received in revised form
15 November 2011
Accepted 2 December 2011
Available online 19 December 2011

Keywords:
Two-layer film
Laser heating
Two-temperature model.

ABSTRACT

The heating processes of a two-layer film assembly of Au padded with Cu irradiated by femtosecond laser pulse are studied using a two-temperature model. It is found that the chosen substantially influence the energy transport, and consequently the temperature variation, and thermal equilibrium time. At the same laser fluence, the different thickness of gold film leads to a change of gold surface temperature. By choosing the thickness of the gold layer in the two-layer film assemblies, the damage threshold of the gold film can be maximized. The results can be used to optimize the damage threshold of gold coating optical components.

1. Introduction

The physics of femtosecond laser heating of gold films has been the focus of scientific research for many years due to the large number of applications [1–4]. Gold coating optical multilayer thin films are important components in many optoelectronic devices. Especially in the field of femtosecond laser, the gold film surface is irradiated by femtosecond laser, the lattice temperature of the substrate metal rises due to the absorption of the incident laser in the gold surface region. Moreover, the lattice temperature rise becomes crucial for the thickness of the metal layer. This is because of larger electron heat flux across the metal layers, which results in nonuniform expansion of each layer. Investigation of the temperature distribution in each layer during laser irradiation becomes important for steady operation. Several papers on the subject have been published in the recent years [5–8]. They suggested that the substrate layer reduced the increase of the surface temperature significantly during femtosecond laser heating. But they did not particularly discuss the effect of the top-layer thickness with regard to the temperature redistribution. In addition, during the processes of interaction between the laser beam and the gold surface, the photo-induced excitation of phonon subsystem effectively interacting with the plasmons and nonlinear optical effects [9,10] are very weak compared with the heating process. So these factors can be ignored.

In here, we performed a series of numerical simulations of femtosecond laser processing of Au film deposited on Cu substrate with 1000 nm thikness, using the finite difference method. The distributions of electron temperature and lattice temperature were considered. The calculated results showed that the thickness of gold layer had a very important influence for the distribution of the film temperature.

2. Mathematical model

The theoretical method to investigate the ultrashort laser-metal interaction is the well-known two-temperature model (TTM). The model has a long history [11]. The TTM describes the evolution of the temperature increase due to the absorption of a laser pulse within the solid and is applied to model physical phenomena like the energy transfer between electrons and lattice occurring during the target–laser interaction [12]. Therefore the expressions for the time evolution of the temperatures read [2,13,14]:

$$C_e\frac{\partial T_e}{\partial t}=\frac{\partial}{\partial x}\left(k_e\frac{\partial T_e}{\partial x}\right)-G(T_e-T_l)+S \tag{1}$$

$$C_l\frac{\partial T_l}{\partial t}=\frac{\partial}{\partial x}\left(k_l\frac{\partial T_e}{\partial x}\right)+G(T_e-T_l) \tag{2}$$

where t is the time, x is the depth, C_e is the electron heat capacity, C_l is the lattice heat capacity, k_e is the electron thermal

* Corresponding authors at: Jilin University Institute of Atomic and Molecular Physics Changchun 130012 China. Tel.: +86 431 85168815; fax: +86 431 85168816.
E-mail addresses: comeongoon@sohu.com (A. Chen), liuhang@jlu.edu.cn (H. Liu).

0030-3992/$ - see front matter © 2011 Elsevier Ltd. All rights reserved.
doi:10.1016/j.optlastec.2011.12.001

conductivity, T_e is the electron temperature, T_l is the lattice temperature, G is the electron lattice coupling factor [15], and S is the laser heat source. The heat source S can be modeled with a Gaussian temporal profile [16]:

$$S=\sqrt{\frac{\beta}{\pi}}\frac{(1-R)I}{t_p\alpha}\exp\left[-\frac{x}{\alpha}-\beta\left(\frac{t-2t_p}{t_p}\right)^2\right] \quad (3)$$

where R is the target reflection coefficient, t_p is the full-width at the half maximum (FWHM) with the linear polarization, α is the penetration depth including the ballistic range, I is the incident energy, $\beta=4\ln(2)$.

The electron heat capacity is proportional to the electron temperature when the electron temperature is less than the Fermi temperature as $C_e=\gamma T_e$ [17] and $\gamma=\pi^2 n_e k_B/2T_F$. n_e is the density of the free electrons, k_B is the Boltzmann's constant. As the temperature changes, the variety of the lattice heat capacity is relatively small, we take it as a constant.

A relationship between the electron relaxation time and electron–electron scattering time $1/\tau_{e-e}=AT_e^2$ and electron-lattice scattering time $1/\tau_{e-l}=BT_l$ for electron temperatures below the Fermi temperature is given by $1/\tau=1/\tau_{e-e}+1/\tau_{e-l}=AT_e^2+BT_l$. The expression for the heat conductivity can be written as $k_e=k_{e0}BT_e/(AT_e{}^2+BT_l)$ [18], k_{e0}, A and B are represent the material constants. Many of the ultrafast laser heating analyses have been carried out with a constant electron–lattice coupling factor G. Due to the significant changes in the electron and lattice temperatures caused by high-power laser heating, $G=G_0(A(T_e+T_l)/B+1)$[4,19] should be temperature dependent. G_0 is the coupling factor at room temperature. The lattice thermal conductivity is therefore taken as 1% of the thermal conductivity of bulk metal since the mechanism of heat conduction in metal is mainly by electrons [3]. As the temperature changes, the variety of the lattice heat conductivity is relatively small, we take it as a constant.

Consider a one-dimensional two-layered thin film, the schematic view of the laser heating is shown in Fig. 1. The thickness of the top layer (Au) is l. The thickness of the substrate layer (Cu) is a constant of 1000 nm.

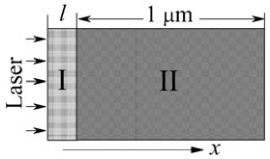

Fig. 1. The schematic of a two-layered film. The thickness of Au is l. The thickness of Cu is 1000 nm.

3. Results and discussion

The typical spatial and temporal distributions of lattice temperature are presented in Fig. 2. The thickness of gold coating layer is 40 nm, 60 nm, 80 nm, and 100 nm, respectively. Accordingly, in the simulation process, the laser wavelength is 800 nm, and the pulse duration is 100 fs. The laser fluence is 2000 mJ/cm^2, and surface reflectivity of gold is $R=0.974$. Table 1[20–24] lists the values of thermal physical parameters of the two noble metals used in these calculations. Fig. 3 shows the variation of the

Table 1
Thermal and optical physical parameters for the two noble metals.

	Au	Cu
G_0 (10^{17} J m^{-3} s^{-1} K^{-1})	0.21	1.0
γ (J m^{-3} K^{-2})	68	97
k_{e0} (J m^{-1} s^{-1} K^{-1})	318	401
C_l (10^6(J m^{-3} K^{-1})	2.5	3.5
α (10^{-9} m)	13.7	12.2
A (10^7 s^{-1} K^{-2})	1.18	1.28
B (10^{11} s^{-1} K^{-1})	1.25	1.23
T_m (°C)	1064	1085

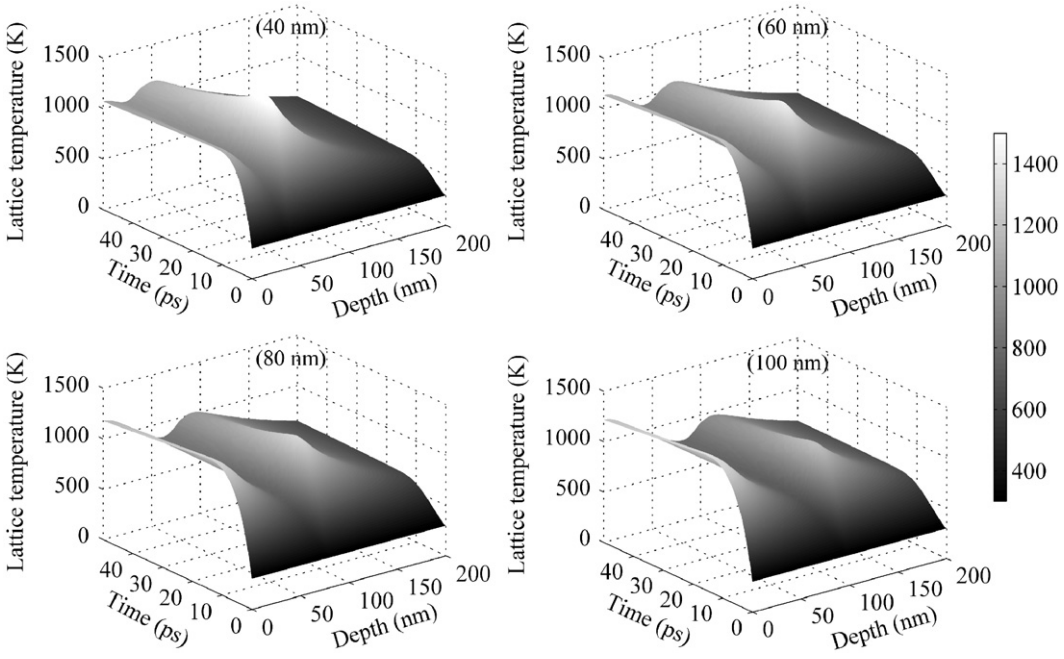

Fig. 2. The distributions of lattice temperatures. The thickness of Au is 40 nm, 60 nm, 80 nm, and 100 nm, respectively. The laser fluence is 2000 mJ/cm^2.

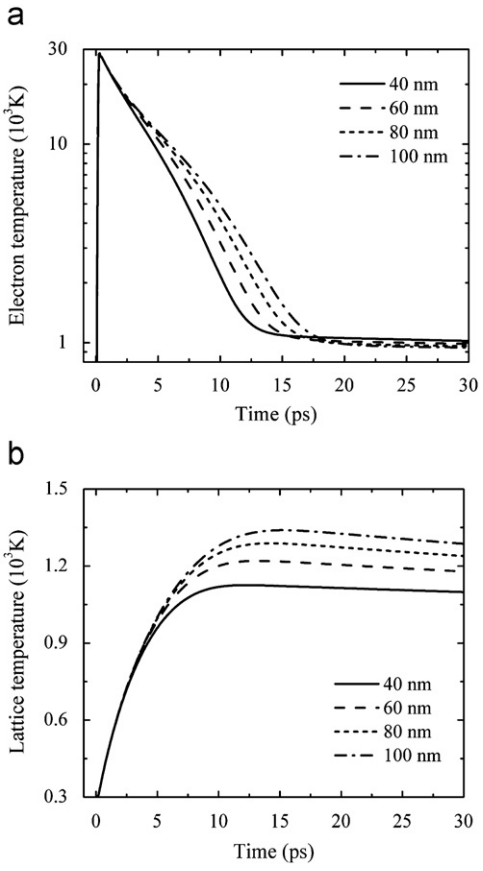

Fig. 3. The variation of surface temperatures with the delay time for the different thickness of Au film: (a) electron temperature; (b) lattice temperature. The thickness is 40 nm (solid line), 60 nm (dashed line), 80 nm (dotted line), and 100 nm (dashed-dotted line), respectively. The laser fluence is 2000 mJ/cm^2.

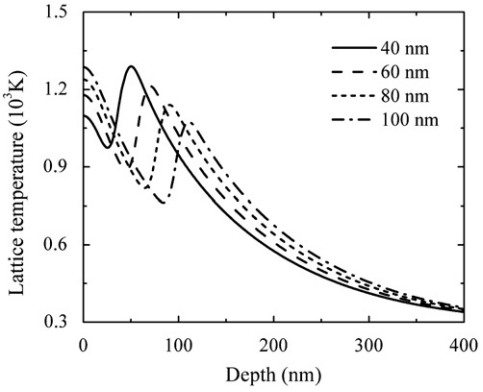

Fig. 4. The variation of lattice temperature with the depth for the different thickness of Au film. The delay time is 30 ps. The laser fluence is 2000 mJ/cm^2.

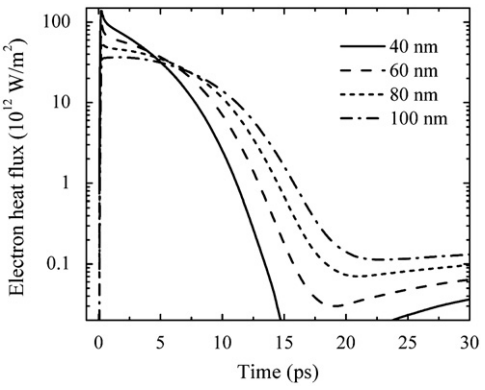

Fig. 5. The variation of electron heat flux with the delay time for the different thickness of Au film. The laser fluence is 2000 mJ/cm^2.

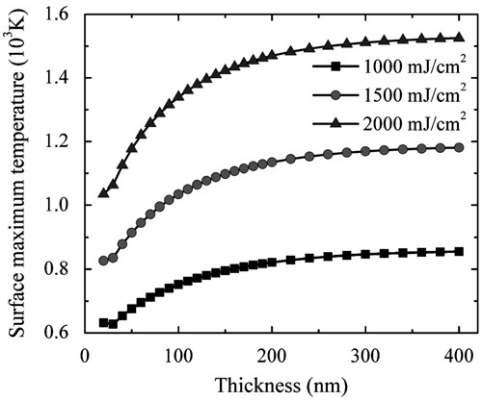

Fig. 6. The surface maximum lattice temperature as a function of the thickness of gold layer for the different laser fluence. The laser fluence is 1000 mJ/cm^2, 1500 mJ/cm^2, and 2000 mJ/cm^2.

electron temperature and lattice temperature at the different delay times up to 30 ps and on the surfaces of four different metal film combinations, respectively. One can see from Fig. 3 (a) that the surface electron temperatures rose rapidly with maximum temperatures being 28.7×10^3 K. Consequently, surface electron temperatures decreased with time due to the electronic thermal diffusion effect in the electron gas, at a short time delay (about 2 ps). The distributions of the surface electron temperature for four different metal combinations were noticeably different. The decay rate of electron temperature of the thicker gold layer was less than that of the thinner gold layer. And relative to the thicker gold layer, the thermal equilibrium times of the thinner gold layer surface was effective reduced. As seen in Fig. 3(b), the surface lattice temperature became higher for thicker gold layer at the thermal equilibrium. At the delay time of 30 ps, the lattice temperature of the different depth is shown in Fig. 4, from where, one can see that, the lattice temperatures changed sharply in the region next to the two-layer interface, like a "sawtooth". This is due to the fact that the electron-lattice coupling factor was considerably higher for Cu substrate than that for the gold layer, causing the redistribution of the deposited laser energy from the gold film layer to the substrate layer, where the energy of the excited electrons coupled more effectively to the lattice vibrations, leading to the preferential lattice heating in the substrate. Cu has a larger electron-lattice coupling factor (Table 1) than Au. In transition from the gold layer to the substrate Cu layer, the electron heat flux is presented in Fig. 5 at the interface. For delays in 0–5 ps range, the electron heat flux of the thinner gold layer was high, and the decay rate was fast. For 5 ps delay and higher, the electron heat flux calculated with the thicker gold layer became higher than that of the thinner gold layer.

With that, we calculated surface maximum lattice temperature for the chosen laser fluence and the thickness of the gold layer. The simulated results are shown in Figs. 6 and 7. In Fig. 6, it is shown that the surface maximum lattice temperature increased dramatically with the increase of gold film thickness when the thickness is less than 200 nm, once the thickness exceeded 200 nm, the surface

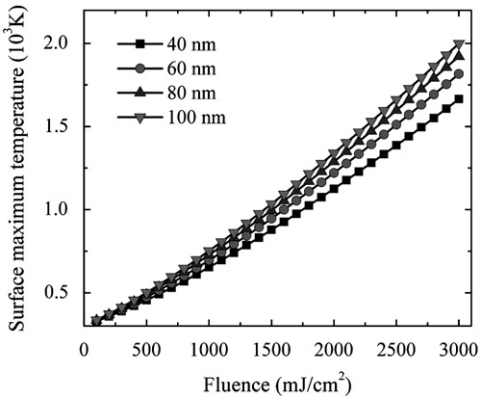

Fig. 7. The surface maximum lattice temperature as a function of laser fluence for the thickness of gold layer. The thickness is 40 nm, 60 nm, 80 nm, and 100 nm.

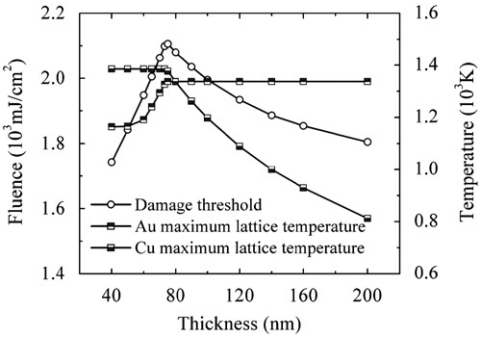

Fig. 8. Damage threshold (left axes), Au layer maximum lattice temperature (right axes), and Cu layer maximum lattice temperature (right axes) recorded for various thickness of Au layer.

maximum lattice temperature almost kept constants with values of 850 K, 1180 K, and 1520 K for three different laser fluences of 1000 mJ/cm^2, 1500 mJ/cm^2, and 2000 mJ/cm^2, respectively. In Fig. 7, for the different thickness of gold layer, the surface maximum lattice temperature increased dramatically with the increase of laser fluence. In the range of the lower laser fluences (0–500 mJ/cm^2), the increasing slope is almost the same for the thin film. The laser fluence increased, while in high laser fluence, the thick film has faster increasing slope.

Finally, we calculated the variation of the damage threshold with the gold thickness. The results are presented in the Fig. 8. Here, we consider that the damage of two-layer film takes place in the regime under the maximum lattice temperature of gold layer or substrate layer reaching the melting point temperature (Table 1). As can be seen, the damage threshold rises with increasing of the gold layer thickness, and maximum temperature of gold layer increases a little, then rises rapidly, however, Cu substrate layer keeps at melting point temperature (1085 °C) at all times, till gold layer thickness arrivers at 75 nm. At the moment, laser fluence of damage threshold is 2106 mJ/cm^2. Maximum lattice temperature of gold layer is 1064 °C. Keep on increasing the thickness of gold layer, damage threshold begins to fall down. However, maximum lattice temperature of Cu substrate layer drops quickly. The Au layer keeps at melting point temperature all along. From above analysis, we find that the Au coating layer of 75 nm thickness is the most optimized system, which can stand a laser fluence up to 2106 mJ/cm^2, is able to attain most damage threshold of Au/Cu thin film assembly.

4. Conclusion

In conclusion, the temporal distributions of the electron temperature and the lattice temperature were calculated on the gold coating copper substrate. For the same total laser fluence, the thickness of the coated layer will lead to the different evolution of electron and lattice temperature. As the thickness of coated layer, the surface electron and lattice temperature increases, however, the electron and lattice temperature of the substrate layer decreases. And, the effect becomes more obvious with the increase of the laser fluence. So, we can find the desired temperature distribution under the femtosecond laser heating by increasing or reducing the thickness of the coated layer. Moreover, the investigated result of the damage threshold showed that the maximum damage threshold can be obtained by changing the thickness of the coated gold. The results can be used to optimize the damage threshold of gold coating optical components (mirror and grating), especially for high-power femtosecond laser system.

Acknowledgement

This project was supported by the National Magnetic Confinement Fusion Science Program of China (grant no. 2010GB104003) and the National Natural Science Foundation of China (grant nos. 10974069 and 11034003).

References

[1] Wang XY, Riffe DM, Lee YS, Downer MC. Time-resolved electron-temperature measurement in a highly excited gold target using femtosecond thermionic emission. Physical Review B 1994;50(11):8016–9.
[2] Ekici O, Harrison RK, Durr NJ, Eversole DS, Lee M, Ben-Yakar A. Thermal analysis of gold nanorods heated with femtosecond laser pulses. Journal of Physics D 2008;41(18):185501–11.
[3] Zhang YW, Chen JK. Ultrafast melting and resolidification of gold particle irradiated by pico- to femtosecond lasers. Journal of Applied Physics 2008;104(5):054910–9.
[4] Huang J, Zhang YW, Chen JK. Ultrafast solid–liquid–vapor phase change of a gold film induced by pico- to femtosecond lasers. Applied Physics A 2009;95(3):643–53.
[5] Thomas DA, Lin Z, Zhigilei LV, Gurevich EL, Kittel S, Hergenroder R. Atomistic modeling of femtosecond laser-induced melting and atomic mixing in Au film – Cu substrate system. Applied Surface Science 2009;255(24):9605–12.
[6] Chen AM, Xu HF, Jiang YF, Sui LZ, Ding DJ, Liu H, Jin MX. Modeling of femtosecond laser damage threshold on the two-layer metal films. Applied Surface Science 2010;257(5):1678–83.
[7] Gao X, Song XW, Lin JQ. Thermal characteristics of double-layer thin film target ablated by femtosecond laser pulses. Chinese Physics B 2011;20(2):024210–5.
[8] Chen AM, Jiang YF, Sui LZ, Liu H, Jin MX, Ding DJ. Thermal analysis of double-layer metal films during femtosecond laser heating. Journal of Optics 2011;13(5):055503–7.
[9] Kityk IV, Ebothe J, Fuks-Janczarek I, Umar AA, Kobayashi K, Oyama M, Sahraoui B. Nonlinear optical properties of Au nanoparticles on indium–tin oxide substrate. Nanotechnology 2005;16(9):1687–92.
[10] Ozga K, Kawaharamura T, Umar AA, Oyama M, Nouneh K, Slezak A, Fujita S, Piasecki M, Reshak AH. Kityk IV. Second order optical effects in Au nanoparticle-deposited ZnO nanocrystallite films. Nanotechnology 2008;19(18). 185709-6.
[11] Anisimov SI, Kapeliovich BL, Perel'man TL. Electron emission from metal surfaces exposed to ultrashort laser pulses. Soviet Physics – JEPT 1974;39(2):375–7.
[12] Corkum PB, Brunel F, Sherman NK, Srinivasan-Rao T. Thermal response of metals to ultrashort-pulse laser excitation. Physical Review Letters 1998;61(25):2886–9.
[13] Hu WQ, Shin YC, King G. Modeling of multi-burst mode pico-second laser ablation for improved material removal rate. Applied Physics A 2010;98(2):407–15.
[14] Gan Y, Chen JK. Integrated continuum-atomistic modeling of nonthermal ablation of gold nanofilms by femtosecond lasers. Applied Physics Letters 2009;94(20). 201116-3.
[15] Allen PB. Theory of thermal relaxation of electrons in metals. Physical Review Letters 1987;59(13):1460–3.
[16] Unal AA, Stalmashonak A, Seifert G, Graener H. Ultrafast dynamics of silver nanoparticle shape transformation studied by femtosecond pulse-pair irradiation. Physical Review B 2009;79(11):115411–7.
[17] Kim J, Na S. Metal thin film ablation with femtosecond pulsed laser. Optics & Laser Technology 2007;39(7):1443–8.

[18] Yamashita Y, Yokomine T, Ebara S, Shimizu A. Heat transport analysis for femtosecond laser ablation with molecular dynamics-two temperature model method. Fusion Engineering and Design 2006;81(8-14):1695–700.
[19] Hopkins PE, Norris PM. Substrate influence in electron–phonon coupling measurements in thin Au films. Applied Surface Science 2007;253(15):6289–94.
[20] Amoruso S, Bruzzese R, Wang X, Nedialkov NN, Atanasov PA. Femtosecond laser ablation of nickel in vacuum. Journal of Physics D 2007;40(2):331–40.
[21] Handbook of Chemistry and Physics, 84th ed. Boca Raton: CRC Press, Boca Raton 2003.
[22] Sanchez JA, Mengüç MP. Melting and vaporization of Cu and Ni films during electron-beam heating. Journal of Applied Physics 2008;103(5). 054316-10.
[23] Yang JJ, Liu WW, Zhu XN. A study of ultrafast electron diffusion kinetics in ultrashort-pulse laser ablation of metals. Chinese Physics 2007;16(7): 2003–10.
[24] Fang RR, Zhang DM, Wei H, Li ZH, Yang FX, Tan XY. Effect of pulse width and fluence of femtosecond laser on electron–phonon relaxation time. Chinese Physics Letters 2007;52(10):3716–9.